A&A 367, 770–779 (2001)
DOI: 10.1051/0004-6361:20000465

Astronomy & Astrophysics

Rapid polarization variations at 20 cm in 0917+624

S. J. Qian[1,2], A. Witzel[1], A. Kraus[1], T. P. Krichbaum[1], and J. A. Zensus[1]

[1] Max-Planck-Institut für Radioastronomie, Auf dem Hügel 69, 53121 Bonn, Germany
[2] Beijing Astronomical Observatory, National Astronomical Observatories (CAS), Beijing 100012, China

Received 15 May 2000 / Accepted 28 November 2000

Abstract. The intraday variations (IDV hereafter) of the total and the polarized flux density observed at 20 cm in 0917+624 (in May 1989) are analysed. It is shown that the IDV can be interpreted in terms of refractive interstellar scintillation. The observed variations are dominated by one scintillating component with a timescale $\tau \approx 0.6$ days and a scintillation index $m \approx 0.04$. In addition, one more scintillating component with a shorter timescale and a smaller scintillation index is needed to improve the fit to the observed Q- and U-light curves. The relationship between the scintillating components and the VLBI components are also discussed. It is shown that Doppler beaming of the 20 cm scintillating components with a Lorentz factor $\gtrsim 7$ may be needed to reduce their intrinsic brightness temperatures significantly below the inverse-Compton limit.

Key words. galaxies: compact – polarization – scattering – radiation mechanisms: non-thermal – quasars: individual: 0917+62

1. Introduction

The nature of IDV observed in compact extragalactic radio sources and blazars (Heeschen et al. 1987; Quirrenbach et al. 1992; Witzel 1992; Krichbaum et al. 1992; Kraus et al. 1999; Kedziora−Chudzcer et al. 1997; Romero et al. 1997; Quirrenbach et al. 2000) has not been fully understood. Owing to their short timescales, the derived apparent brightness temperatures are mostly in the range of $10^{16}-10^{18}$ K (and can in extreme cases even reach 10^{21} K), severely violating the inverse Compton limit (Kellermann & Pauliny−Toth 1969). Many models (both intrinsic and extrinsic) have been proposed to explain this phenomenon (Wagner & Witzel 1995; Qian 1994a).

Refractive interstellar scintillation (RISS, Rickett 1990; Rickett et al. 1995; Qian 1994a,b; Qian et al. 1995) has been suggested to explain intraday variations, assuming that IDV sources contain very compact components of angular size $\lesssim 50-100\,\mu$as and a distance of the scattering screen (or the scale height of the interstellar scattering medium) of $\lesssim 0.2-0.5$ kpc. Recently, extremely rapid variations, with timescales of hours, were observed in a few sources (for example, PKS 0405−385, PKS 1519−273 and J1815+3845) and have been interpreted in terms of refractive interstellar scintillation (Kedziora−Chudczer et al. 1997; Macquart et al. 2000; Dennett-Thorpe & de Bruyn 2000). In these cases the angular sizes of the scintillating components are derived to be $\sim 5-20\,\mu$as and the distance of the scattering screen then needs to be $\sim 20-50$ pc. Generally, an RISS interpretation can avoid the Compton catastrophe problem. However, for the IDV events observed in PKS 0405−385 and PKS 1519−273, the derived apparent brightness temperatures are in the range of $\sim 10^{14}-10^{15}$ K. If these high brightness temperatures are due to Doppler beaming, the required Lorentz factors of bulk motion would reach $\sim 100-1000$.

In contrast, the correlated optical-radio intraday variations observed in the BL Lac object 0716+714 (Wagner & Witzel 1995; Qian et al. 1996; Wagner et al. 1996) imply that this IDV event is due to an intrinsic mechanism, because RISS cannot produce optical variations. Among the different intrinsic models, shock models have been proposed to explain the IDV phenomenon (Qian et al. 1991; Marscher 1998; Spada et al. 1999). It was suggested that in some specific geometries the apparent size of IDV components may be much larger than those derived from the light-travel-time arguments, and by applying a Lorentz factor of ∼10–20, the high brightness temperatures ($\sim 10^{16}$–10^{18}) observed could be explained.

Although the most extreme IDV events are likely to be caused by refractive interstellar scintillation, it might be difficult to explain all IDV events in this way (Gabuzda et al. 1999; Marscher 1996; Kochanev & Gabuzda 1998). Therefore, it is most important to distinguish between IDV as a phenomenon intrinsic to compact radio sources and IDV which is primarily due to scintillation. However, the disentanglement of the intrinsic intraday variations

Send offprint requests to: A. Witzel

from scintillation is very difficult for IDV events of small-amplitude fluctuations (less than ∼10–15%).

Intraday variations of total flux density have been studied intensively, but the properties of IDV polarization variations have not been investigated thoroughly (Quirrenbach et al. 1989). Qian et al. (1991) used a shock model to explain the intraday polarization variations observed in 0917+624 in the IDV event of December 1988. It was shown that a two-component model (one steady component and one shock with a variable polarization degree and polarization angle) could explain the complicated polarization variations (anti-correlation between the total and polarized flux density and a polarization angle swing of ∼180°). They found that the polarization of the shock component was nearly perpendicular to that of the steady component and the polarization degree and polarization angle of the shocked region were required to vary only in a narrow range.

Rickett et al. (1995) have shown that the 2–11 cm flux variations observed in the IDV of May 1989 in 0917+624 could be explained by refractive interstellar scintillation and the VLBI core might be the main scintillating component. But they found that the 20 cm flux density variations are not as well correlated with those at 2–11 cm as predicted by scintillation theory. They suggested that the dominant scintillating component at 20 cm is a more extended component (not the VLBI core). They have also attempted to interpret the intraday polarization variations observed at 6 cm in 0917+624 in terms of refractive scintillation. Since RISS cannot produce variations of the polarization degree and polarization angle of a single scintillating component, two or more scintillating components were required to explain the complicated polarization variations observed in 0917+624 at high frequencies. In addition, Qian (1994a,b) applied multi-frequency structure functions (Blandford et al. 1986; Qian et al. 1995) to investigate the possibility of interpreting the IDV in 0917+624 and other sources in terms of refractive interstellar scintillation.

In this paper, we discuss the rapid polarization variations observed at 20 cm in 0917+624 and suggest that the polarization variations must be due to more than one component.

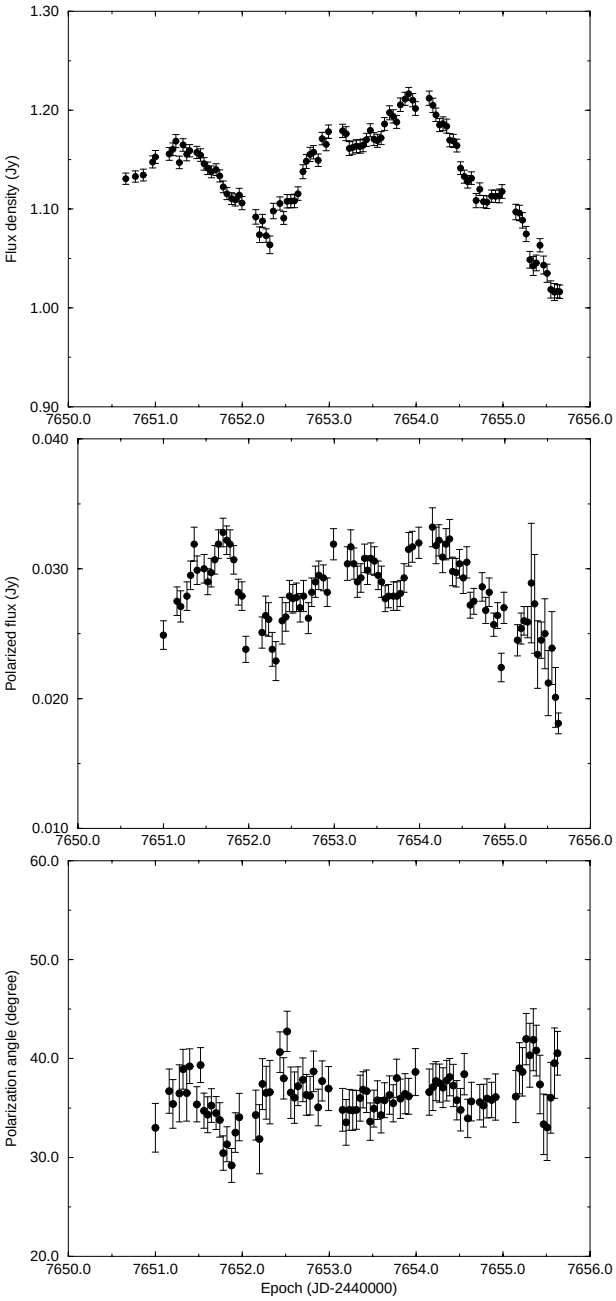

Fig. 1. Intraday variations observed at 20 cm in 0917+624 (May 1989, JD2447650.0–2447656.0, from top to bottom): total flux density I (Jy), polarized flux density P (Jy) and polarization angle χ (°). (Unsmoothed data)

2. Polarization observations at 20 cm

2.1. Description

In May 1989 (JD2447650–2447656), multifrequency flux density and linear polarization observations were carried out at five frequencies (1.4, 2.7, 5, 8.3 and 15 GHz) using the VLA (Quirrenbach et al. 2000). Here we mainly investigate the variations observed at 20 cm and discuss their origin. The light curves of the total flux density (I), polarized flux density (P) and polarization angle (χ) are shown in Fig. 1. The typical interval between samples is ∼0.04 days and the observational errors are approximately: 7–8 mJy (total flux density), 1–1.5 mJy (polarized flux density) and 2–3° (polarization angle). In order to remove high frequency noise due to observational uncertainties, in the following discussions we will use five-point running averages for the three quantities.

2.2. Characteristics of the variations

The main properties of the variations observed at 20 cm can be described as follows.

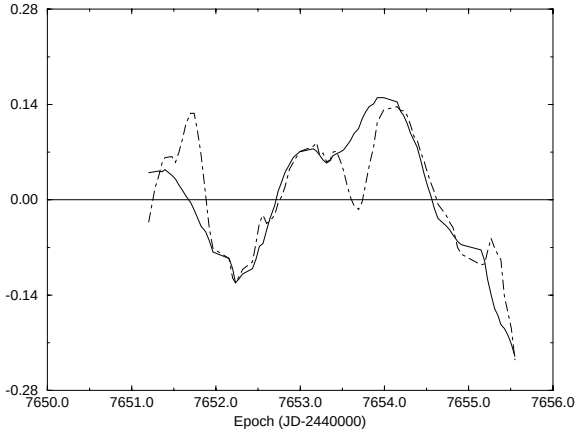

Fig. 2. The observed fractional variations of the total flux density ($\Delta I(t)/\overline{I}$, solid line) and the polarized flux density ($\Delta P(t)/\overline{P}$, dot-dashed line) ($\overline{I} = 1.137$ Jy, $\overline{P} = 28.54$ mJy). The fractional variations of the total flux density have been scaled up by a factor of 2.36. A clear correlation between ΔP and ΔI is visible. (Smoothed data)

- The mean values of the total flux density, polarized flux density and the polarization angle are 1.137 Jy ($\bar{I}$), 28.5 mJy ($\bar{P}$) and 36.°3 ($\bar{\chi}$) with their standard deviations being 0.045 Jy, 2.3 mJy and 1.°8 respectively;
- The variability indices of the fluctuations of the total and polarized flux density are 5.7% and 11.6%, respectively, showing that the polarized flux density has a much larger fractional variability amplitude;
- The polarization angle varies only in a very narrow range. Its maximal deviation from the mean value is only about 5–6° (see Fig. 1), but the variations appear systematic;
- During about half of the observing period (∼2.3 days), the fractional variations of the polarized flux density are precisely proportional to those of the total flux density. This can be seen more clearly in Fig. 2, where the fractional variations of the total flux density ($\Delta I(t)/\overline{I}$) and the polarized flux density ($\Delta P(t)/\overline{P}$) are shown. ($\Delta I(t) = I(t) - \overline{I}$ and $\Delta P(t) = P(t) - \overline{P}$). For the period when the proportionality holds the correlation coefficient between $\Delta P(t)$ and $\Delta I(t)$ reaches ∼0.97.

The last two of the properties listed above are considerably different from those observed at the higher frequencies. For example, at 5 GHz both a correlation and anti-correlation between the variations of the total and polarized flux density, a rapid transition between the two kinds of relationship and relatively large polarization angle swings (20°–40°) were observed (Qian et al. 1991).

In the following, we will show that the characteristics of the intraday polarization variations observed at 20 cm can be explained in terms of refractive interstellar scintillation with two scintillating components in the source.

3. Two-component model

In this section we consider a two-component model. A two-component model consisting of one steady and one variable component can be generally applied to study different kinds of variability, extrinsic or intrinsic. However, intrinsic variations usually imply that the source polarization itself is variable.

As we pointed out in the last section, during half of the observing period, the fractional variations of the polarized flux density are proportional to those of the total flux density (Fig. 2). In other words, the observed quantities $\Delta P(t)$ and $\Delta I(t)$ are highly correlated. This suggests that the polarization variations observed at 20 cm are dominated by one scintillating component. Therefore, as a first approximation, we can use a two-component model (one scintillating and one steady component) to explain the observed variations.

3.1. Polarization parameters

In the case of a two-component model the basic equations for the Stokes parameters $I(t)$, $Q(t)$ and $U(t)$ are (Rickett et al. 1995):

$$I(t) = I_0 + \Delta I(t) \tag{1}$$

$$Q(t) = Q_0 + \Delta I(t) m_{\rm q2} \tag{2}$$

$$U(t) = U_0 + \Delta I(t) m_{\rm u2}\,, \tag{3}$$

where

$$I_0 = I_{10} + I_{20} \tag{4}$$

$$Q_0 = I_{10} m_{\rm q1} + I_{20} m_{\rm q2} \tag{5}$$

$$U_0 = I_{10} m_{\rm u1} + I_{20} m_{\rm u2} \tag{6}$$

$$m_{\rm q1} = p_1 \cos 2\chi_1 \tag{7}$$

$$m_{\rm q2} = p_2 \cos 2\chi_2 \tag{8}$$

$$m_{\rm u1} = p_1 \sin 2\chi_1 \tag{9}$$

$$m_{\rm u2} = p_2 \sin 2\chi_2\,. \tag{10}$$

$\Delta I(t)$ is the observed fluctuation of the total flux density caused by scintillation. (I_{10}, p_1, χ_1) and (I_{20}, p_2, χ_2) are the flux density, polarization degree and polarization angle of the steady and the scintillating component (designated as S_1 and S_2), respectively. All of these parameters are assumed to be constants. (According to scintillation theory, in the case of isotropic scattering, RISS cannot produce significant variations in the polarization degree and polarization angle of the scintillating component.) $I_0 \equiv \bar{I} = 1.137$ Jy.

It can be seen that, taking the observed values for ($\Delta I(t)$, $Q(t)$, $U(t)$), in the Eqs. (2) and (3), there are only four unknown constants (Q_0, U_0, $m_{\rm q2}$, $m_{\rm u2}$), so we can use the entire observational data to find a solution for these parameters by a least-square-fit, which minimizes

the mean square difference between the modeled and the observed ($Q(t)$, $U(t)$).
The appropriate parameters are found to be:
$Q_0 = 8.46\,\mathrm{mJy}$, $U_0 = 27.14\,\mathrm{mJy}$,
($p_0 = 0.0250$, $\chi_0 = 36\overset{\circ}{.}34$),
$m_{\mathrm{q}2} = 0.0180$, $m_{\mathrm{u}2} = 0.0412$,
($p_2 = 0.0449$, $\chi_2 = 33\overset{\circ}{.}2$).
It can be seen that the polarization angle derived for the scintillating component (S_2) is very close to that of the steady component, so the fluctuations due to the scintillation of this component cannot produce a significant contribution to the observed variations of the polarization angle.

Using these values, we can derive the modeled Stokes parameters $Q_{\mathrm{m}}(t)$ and $U_{\mathrm{m}}(t)$ from Eqs. (2) and (3). The modeled polarized flux density $P_{\mathrm{m}}(t)$ and polarization angle $\chi_{\mathrm{m}}(t)$ can then be derived through the relations: $P_{\mathrm{m}}(t) = [Q_{\mathrm{m}}(t)^2 + U_{\mathrm{m}}(t)^2]^{\frac{1}{2}}$, $Q_{\mathrm{m}}(t) = P_{\mathrm{m}}(t)\cdot\cos 2\chi_{\mathrm{m}}(t)$ and $U_{\mathrm{m}}(t) = P_{\mathrm{m}}(t)\cdot\sin 2\chi_{\mathrm{m}}(t)$.

3.2. Model-fitting results

3.2.1. Modeled light curves for polarized flux and polarization angle

The results of model-fitting to the observed polarized flux density and polarization angle are shown in Fig. 3. It can be seen that the two-component model can fit most of the light curve of the observed polarized flux density. However, there are two features (at epochs JD2447651.7 and JD2447653.6), which deviate significantly from the modeled light curve. Their maximal deviations are $\sim$3.5 mJy and $\sim$3.0 mJy (with a significance level of $\sim 3\sigma$), respectively.

Since the derived polarization angle of the scintillating component (S_2) is different from that of the steady component by only $\sim 3^\circ$, the modeled light curve of the polarization angle is almost a straight line. Therefore, the observed deviations of the polarization angle (and also the residual features in the observed light curve of the polarized flux density) could be due to additional variable components.

3.2.2. Modeled light curves for Q and U

The model-fits to the Q- and U-light curves are shown in Fig. 4. The root-mean-square fitting error is $\sim$1.76 mJy (for Q) and $\sim$1.17 mJy (for U).

It can be seen that the variations in Q closely follow the variations in the polarization angle, i.e. Q increases (decreases) while the polarization angle decreases (increases). This characteristic can be easily understood, because for this IDV event the Stokes parameter Q ($\propto \cos(2\chi)$ and $2\chi \approx 72^\circ$) is most sensitive to the variations of the polarization angle. In the observed Q-light curve the feature at epoch JD2447651.75 is clearly deviating from the model[1]. This feature corresponds to the maximal deviations in the light curve of the polarization angle (Fig. 3). This may imply that there is an additional component, which mainly causes the observed variations of the polarization angle.

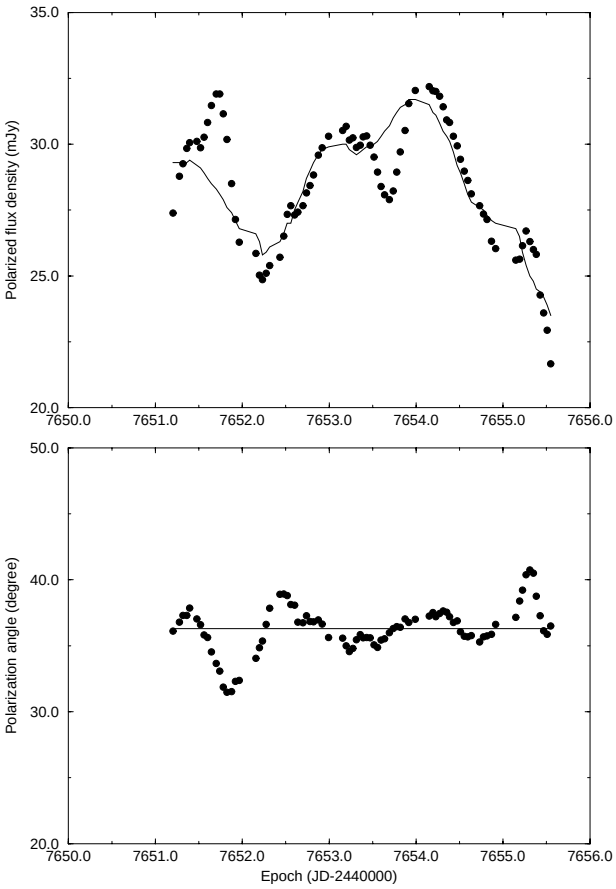

Fig. 3. The model-fits to the polarized flux density and polarization angle observed at 20 cm by a two-component model (one steady and one scintillating component). Points – observation, solid line – model

In the observed U-light curve there are also a few features (including that at epoch JD2447653.6) which significantly deviate from the model. In contrast to Q, the Stokes parameter U is not sensitive to variations in the polarization angle. Thus the feature at epoch JD2447653.6 appeared with a slight variation of the observed polarization angle, but the associated variations in both U and polarized flux density P are significant.

From the model-fitting results given above, we conclude that, one more scintillating component may be needed to explain the residual variations in the flux density and polarization with a smaller modulation amplitude and a shorter time scale.

[1] The root-mean-square fitting error for the interval JD2447651.20–2447653.20 is $\sim$2.29 mJy, significantly larger than that for the whole event.

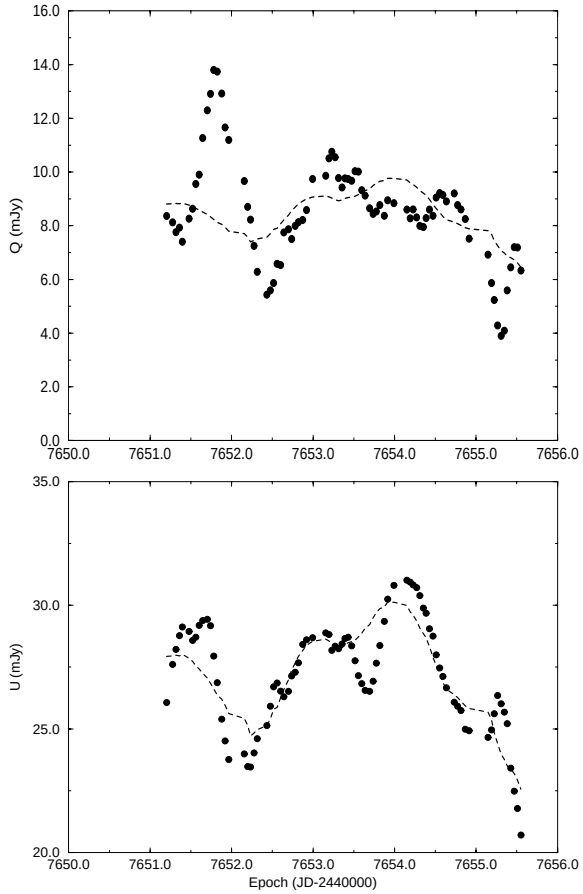

Fig. 4. The model-fits to the Q- and U-light curves with the same model as in Fig. 3

4. Three-component model

We now consider a three-component model: one steady component and two scintillating components (S_2 and S_3). In this case the basic equations for the Stokes parameters (see Eqs. (1)–(3)) should be correspondingly modified to include the contributions from the second scintillating component as follows.

$$I(t) = I_0 + \Delta I_2(t) + \Delta I_3(t) \tag{11}$$

$$Q(t) = Q_0 + \Delta I_2(t) m_{\rm q2} + \Delta I_3(t) m_{\rm q3} \tag{12}$$

$$U(t) = U_0 + \Delta I_2(t) m_{\rm u2} + \Delta I_3(t) m_{\rm u3}\,. \tag{13}$$

In these equations the quantities I_0, Q_0 and U_0 may be regarded as known constants which have been determined in the two-component model. We then have four unknown constants ($m_{\rm q2}$, $m_{\rm u2}$, $m_{\rm q3}$, $m_{\rm u3}$) and one time-series $\Delta I_2(t)$ (or $\Delta I_3(t)$) to be solved. Basically, this is a problem of decomposing the observed light curve $\Delta I(t)$ into its two sub-components, $\Delta I_2(t)$ and $\Delta I_3(t)$. In general, there might be no unique solution for these parameters. In dealing with the modeling of the polarization variation at 6 cm, Rickett et al. (1995) proposed a simplified model, in which a simple time offset between the time-series of the two scintillating components was assumed. Therefore, the time-series $\Delta I_2(t)$ and $\Delta I_3(t)$ were obtained from $\Delta I(t)$ through a procedure of Fourier and inverse-Fourier transformation. The remaining four parameters ($m_{\rm q2}$, $m_{\rm u2}$, $m_{\rm q3}$, $m_{\rm u3}$) were then determined from Eqs. (11)–(13) by a least-square method.

However, in the present case, the angular sizes of the two 20 cm scintillating components are significantly different and the relationship between the two time-series may not reasonably be represented by a simple time offset. Convolution of the scintillation pattern with the brightness distribution of the two components may also be involved. Therefore, we have to look for an alternative way to solve the problem for decomposing the observed light curve $\Delta I(t)$ and consider some particular solutions.

On the basis of a comparison between the variations at 20 cm and at 6–11 cm, Rickett et al. (1995) pointed out that the source component causing the scintillation at 20 cm is not the source component causing the scintillation at 2–11 cm. They suggested that the scintillating component at 2–11 cm is associated with the VLBI compact core (component-A, following the designation by Standke et al. 1996), while the 20 cm scintillating component is associated with a more extended component-D. This scheme of two scintillating components is just consistent with our analysis of the polarization variability observed at 20 cm, if we assume that the second 20 cm scintillating component is associated with the compact core. Since the core component has a smaller angular size and is optically thick at 20 cm, its scintillation could have a shorter timescale and a smaller amplitude. This is consistent with the properties required for the second scintillating component.

This reasonable assumption provides the possibility that the 20 cm time-series caused by the second scintillating component (i.e. $\Delta I_3(t)$) can be obtained by smoothing the 11 cm time-series with an appropriate time constant ($\Delta\tau$) and scaling with an appropriate amplitude factor ($R_{\rm A}$). Thus the time-series $\Delta I_2(t)$ can also be determined through Eq. (11). Using the Eqs. (12), (13), we can then solve the polarization parameters ($m_{\rm q2}$, $m_{\rm u2}$) and ($m_{\rm q3}$, $m_{\rm u3}$) by a least-square method.

We consider the following cases, in which a model time-series for $\Delta I_3(t)$ is obtained from the smoothing of the 11 cm time-series with $\Delta\tau = 0.5$ days and $R_{\rm A} = 0.8$, and try to improve the model-fitting to the observed Q- and U- light curves. The choice of the values for $\Delta\tau$ and $R_{\rm A}$ is based on the consideration: (1) Component S_3 has a larger angular size at 20 cm than at 11 cm and its scintillation at 20 cm occurs in the strong scattering regime; (2) the scintillation timescale of component S_3 is significantly less than that of component S_2; (3) the modulation amplitude due to component S_3 is significantly smaller than that due to component S_2 (see Table 1 below).

– Case-1: The model 20 cm time-series $\Delta I_3(t)$ is directly used to solve the four polarization constants by a least-square method. It is found that $m_{\rm q2} \approx m_{\rm q3}$ and $m_{\rm u2} \approx m_{\rm u3}$, with a difference less than 15%. The model-fitting to the observed light curves is almost completely

Table 1. Parameters derived for the two scintillating components at 20 cm

Parameter	Component S_2	Component S_3
σ(mJy)	48.0	22.5
τ(day)	0.63	0.34
$m_{\rm obs}$	0.042	0.020
$V_\perp$(km s^{-1})	38.5	38.5
$\theta_{\rm s}(\mu$as)	120	65
VLBI-component	D	A
$\theta_{\rm VLBI,6\,cm}$(mas)	1.3	0.22
$S_{\rm VLBI}$(mJy)	400	300
$m_{\rm p}(=\sigma/S_{\rm VLBI})$	0.12	0.075
SM($10^{-3.5}$ m$^{-20/3}$ kpc)	0.26	0.26
$\theta_{\rm d}(\mu$as)	98.7	98.7
$\theta_{\rm f}(\mu$as)	15.3	15.3
$m_{\rm R}$	0.18	0.37
$S_{\rm c}(=\sigma/m_{\rm R}$, mJy)	267	60.8
$\eta_{\rm c}(=S_{\rm c}/S_{\rm VLBI})$	0.67	0.20
$T_{\rm b}(10^{12}$ K)	3.7	2.8
$\delta(H_0 = 100$ km s$^{-1}\cdot$Mpc)	7.8	7.8
$T_{\rm b,int}(10^{11}$ K)	4.7	3.6

similar to that by the two-component model. Therefore, this case is essentially equivalent to the two-component model (with one scintillating component) presented in Sect. 3. This may imply that the compact core at 20 cm is shifted along the jet by optical depth effects, so we consider two more cases;

– Case-2: The model time-series $\Delta I_3(t)$ is offset by –0.40 days, making the prominent residual polarization feature at epoch JD2447651.75 (see Fig. 4) coincident with a minimum in the model light curve. This choice of the time offset is mainly to obtain a reasonable polarization degree (less than ∼10% or so) for the scintillating component S_3. The four polarization constants are determined to be: $m_{\rm q2} = 0.0094$, $m_{\rm u2} = 0.0422$ (or $p_2 = 0.043$, $\chi_2 = 38\overset{\circ}{.}7$); $m_{\rm q3} = -0.0171$, $m_{\rm u3} = 0.0312$ (or $p_3 = 0.036$, $\chi_3 = -30\overset{\circ}{.}6$);
– Case-3: The model time-series $\Delta I_3(t)$ is offset by +0.15 days, making the prominent residual polarization feature at JD2447651.75 coincident with a maximum in the model light curve. The four polarization constants are determined to be: $m_{\rm q2} = 0.0147$, $m_{\rm u2} = 0.0431$ (or $p_2 = 0.046$, $\chi_2 = 35\overset{\circ}{.}6$); $m_{\rm q3} = 0.0336$, $m_{\rm u3} = 0.0541$ (or $p_3 = 0.064$, $\chi_3 = 29\overset{\circ}{.}1$).

It can be seen that for the latter two cases, the polarization constants $m_{\rm q2}$ and $m_{\rm u2}$ for the scintillating component S_2 are close to the values obtained in the two component model. This confirms the dominance of the scintillation caused by component S_2. For both cases (case-2 and case-3)the model fitting to the light curves of Q and U (or $I_{\rm p}$ and χ) is improved over the two component model, especially for the Q- and PA-light curves during the period JD2447651.5–2447653.0. The main difference between case-2 and case-3 is that in case-2 the scintillating component S_3 has a polarization angle different from that of the steady component by ∼63°, while in case-3 the difference

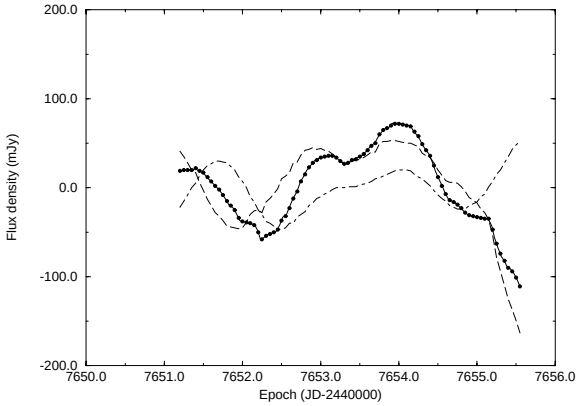

Fig. 5. Decomposition of the flux density fluctuation observed at 20 cm: dashed line – scintillating component S_2, dot-dashed line – scintillating component S_3, solid line – sum of the two components, points – observation

in polarization angle is less than 10°. This is related to the choice of the time offset for the model time-series: in case-2 the prominent residual feature (at epoch JD2447651.7) in the Q-light curve corresponds to negative deviations in the flux density, while in case-3 it corresponds to positive deviations in the flux density.

Since the improvement of the model-fitting in case-2 is very similar to that in case-3, only the results for case-3 are presented here. In Fig. 5 we show the decomposition of the observed flux density fluctuations. The model fitting to the Q- and U-light curves and to the polarized flux density and polarization angle are shown in Figs. 6 and 7, respectively. From the comparison of Fig. 6 with Fig. 4 it can be seen that the fit with the 3-component model is improved over the 2-component model, mainly for the interval JD2447651.20–2447653.20. The root-mean-square fitting error is reduced by about 20% for Q, but only about 10% for U.

The structure functions for the variations caused by the two scintillating components are shown in Fig. 8. From the structure functions, it is found that the scintillation from the component S_2 has a time scale of 0.63 days and its root-mean-square fluctuation of flux density (standard deviation σ) is ∼48.0 mJy (or modulation index $m_{\rm obs,2} \approx 0.042$ (normalized by the total flux density of the source)). The scintillation from the component S_3 has a shorter time scale of 0.34 days and a smaller fluctuation amplitude of ∼22.5 mJy (or modulation index $m_{\rm obs,3} \approx 0.020$). In addition, the linear part of both structure functions have a slope of ∼1.7, which might imply that the interstellar medium consists of two components: the continuous medium and a thin screen (Qian & Zhang 1996).

We point out that the two time-series ($\Delta I_2(t)$ and $\Delta I_3(t)$, Fig. 5) derived for the scintillating components S_2 and S_3 are weakly correlated with a correlation coefficient of <0.4. This can be explained as they are respectively associated with the VLBI components D and A, which are separated along the jet by ∼5 mas. During the period

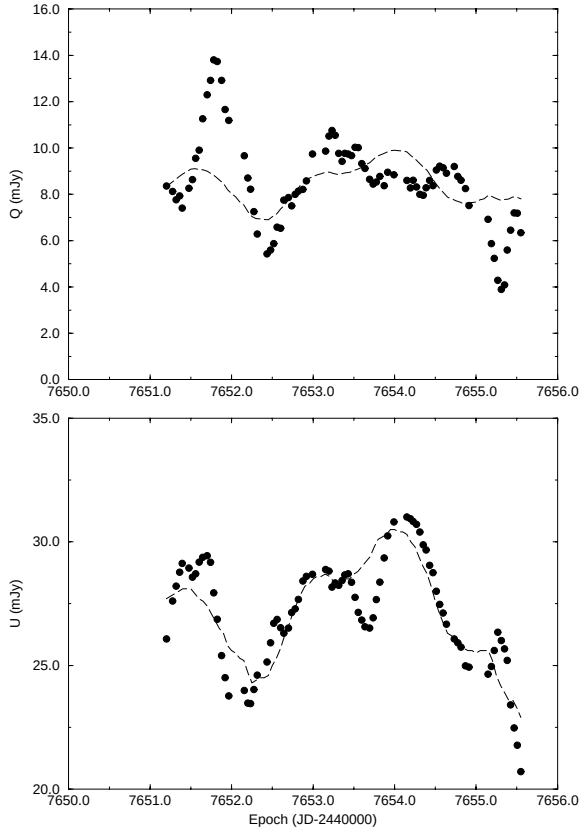

Fig. 6. The model-fitting to the observed Q- and U-light curves by the three-component model. Points – observation, dashed line – model (case–3)

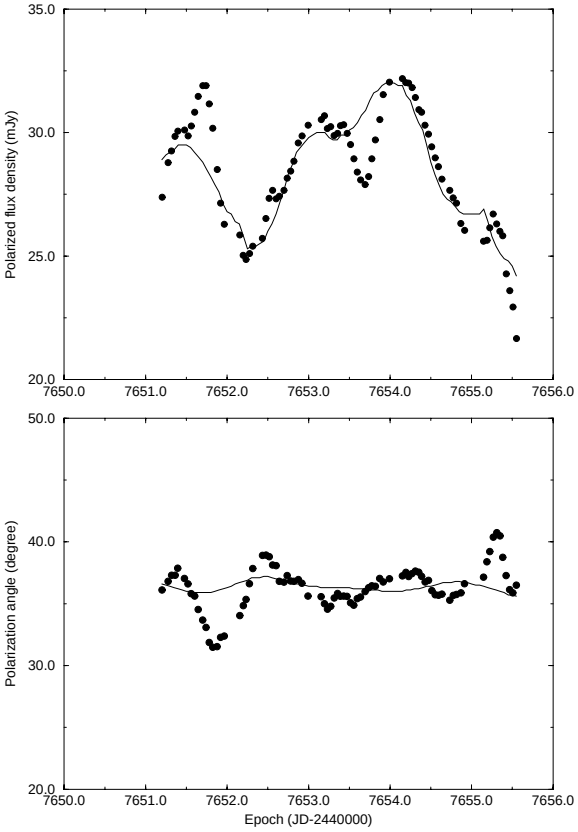

Fig. 7. The model-fitting to the observed polarized flux density and polarization angle light curves observed at 20 cm. Points – observation, solid line – model

of observation, the direction of the projected Earth velocity (position angle $\sim -(18\text{–}25°)$) [2] was very closely to the jet direction (position angle $\sim -20°$). Thus the separation of the two scintillating components is much larger than the angular scale of the scattering pattern (~ 0.1 mas, see below) and no significant correlation between the two time-series should be expected.

5. Discussion

In the previous section, we analysed the 20 cm IDV event in the scheme of a three-component model. Now we further discuss the relationship between the two scintillating components and their corresponding VLBI components. More information can be obtained for the source components and the interstellar medium in the direction towards 0917+624.

VLBI observations made by Standke et al. (1996) at multiple frequencies (1.7, 2.3, 5, 8.3 and 22 GHz during 1988–1993) have shown that in 0917+ 624 there are seven components, designated as A to G. Components C, E, F and G are probably too extended to scintillate at

[2] Here we assume that the scattering medium is at rest in the Local Standard of Rest (LSR) and the relative velocity between the Earth and the scattering medium is due to the Earth's orbital motion around the Sun and the motion of the solar system barycenter with respect to the LSR.

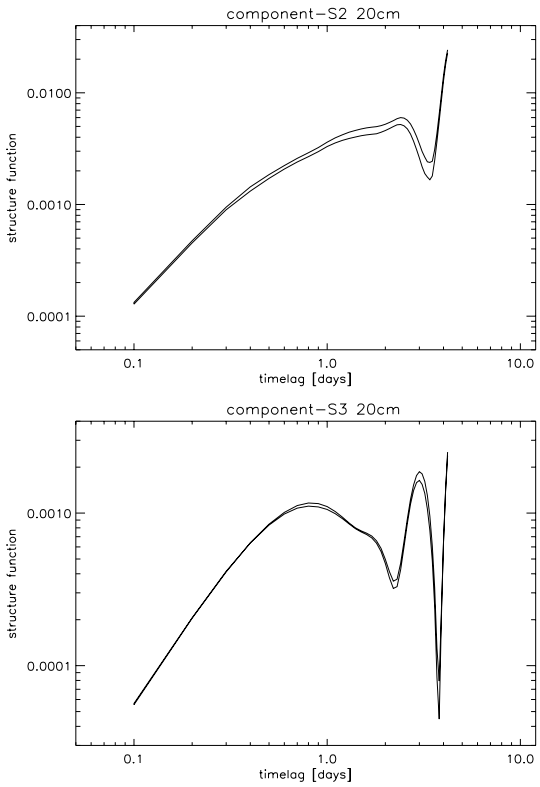

Fig. 8. Structure functions for the two 20 cm scintillating components S_2 and S_3

20 cm. Component-A is the most compact (VLBI core) with its turnover frequency at ∼7 GHz. Standke et al. (1996) pointed out that the optically thick spectral index of the component-A is much less than 2.5 and suggested that component-A is inhomogeneous and might be a blend of underlying subcomponents which are not resolved. As Rickett et al. (1995) suggested, the intraday variations at 2–11 cm are due to scintillation of the most compact component-A, in which there is a subcomponent having an angular size of ∼70 μas with ∼44% of the total flux density of the source at 6 cm. As shown above, we have suggested that the 20 cm scintillating component S_3 is associated with this VLBI component. According to Standke et al. its flux density at 20 cm is about 300 mJy ($S_{\rm VLBI,3}$). The VLBI component-D, which is associated with the scintillating component S_2, has a flux density ∼400 mJy ($S_{\rm VLBI,2}$) at 20 cm. We should point out that the 20 cm flux densities were derived by Standke et al. by decomposing the integral spectrum and could have large uncertainties.

In the following, we will use these values to estimate some physical parameters for the VLBI-components and the interstellar medium. The formulae relevant to the derivation of the scintillation parameters are given by Goodmann (1997) and Narayan (1992), assuming that the scattering medium is characteristic of Kolmogolov turbulence.

– (1) Scattered path length and transition frequency
First, as in the scintillation model of Rickett et al., the scattered path length d is assumed to be 0.2 kpc and the frequency of transition ($\nu_{\rm tr}$) from weak to strong scattering is assumed to be ∼ 4 GHz;

– (2) Scattering measure
Using the values given above, the scattering measure SM (in units of $10^{-3.5}$ m$^{-\frac{20}{3}}$kpc) of the interstellar scattering medium can be determined[3]:

$$SM \approx 1.31\ 10^{-3}\Big(\frac{\nu_{\rm tr}}{\rm GHz}\Big)^{\frac{17}{6}}\Big(\frac{d}{\rm kpc}\Big)^{-\frac{5}{6}}. \quad (14)$$

We obtain $SM \approx 0.26$.

– (3) Scattering angle
The scattering angle $\theta_{\rm sc}$ (μas) of the medium is given by the formula:

$$\theta_{\rm sc} \approx 2.93\,\Big(\frac{\nu}{10\ {\rm GHz}}\Big)^{-2.2} SM^{0.6}. \quad (15)$$

Having the value for SM, we can estimate the scattering angle at 20 cm (ν = 1.4 GHz): $\theta_{\rm sc} \approx 98.7$ μas. The Fresnel angle $\theta_{\rm f}$ (μas) is given by:

$$\theta_{\rm f} \approx 2.57\Big(\frac{\nu}{10\ {\rm GHz}}\Big)^{-0.5}\Big(\frac{d}{\rm kpc}\Big)^{-0.5}. \quad (16)$$

[3] Below, we will use the formulae given by Goodmann (1997).

We obtain $\theta_{\rm f} \approx 15.3$ μas. Thus, $\theta_{\rm sc} \gg \theta_{\rm f}$ and the scintillation at 20 cm occurs in the strong scattering regime.

– (4) Angular sizes of the scintillating components
The observed timescales τ (days) of the scintillating components are related to their effective size $\theta_{\rm eff}(\mu{\rm as})$, the scattered path length d and the projected relative velocity $V_\perp$(km s^{-1}) between the Earth and the scattering screen:

$$\tau \approx 0.29\,\Big(\frac{\theta_{\rm eff}}{10\ \mu{\rm as}}\Big)\Big(\frac{d}{\rm kpc}\Big)\Big(\frac{V_\perp}{30\ {\rm km\ s^{-1}}}\Big)^{-1}. \quad (17)$$

Here the effective angular size of the scintillating components is given by:

$$\theta_{\rm eff} \approx [{\theta_{\rm s}}^2 + (0.71\theta_{\rm sc})^2]^{0.5}; \quad (18)$$

$\theta_{\rm s}(\mu{\rm as})$ is the angular size of the scintillating components. From the time scales (τ_2 and τ_3) derived in the previous section for the two scintillating components S_2 and S_3, the effective angular sizes can be estimated to be $\theta_{\rm eff,2} \approx 139\,\mu$as ($S_2$) and $\theta_{\rm eff,3} \approx 75\,\mu$as ($S_3$). (During the observing period the projected velocity of the Earth relative to the scattering medium is about 38.5 km s^{-1}). Since $\theta_{\rm eff,2} \gg \theta_{\rm sc}$, the intrinsic angular size of the scintillating component S_2 can be estimated from Eq. (18) to be $\theta_{\rm s,2} \approx 120$ μas. For the scintillating component S_3, $\theta_{\rm eff,3} \approx 0.71\,\theta_{\rm sc}$, its intrinsic angular size cannot be estimated from Eq. (18); we assume that $\theta_{\rm s,3} \approx \frac{\tau_3}{\tau_2}\theta_{\rm s,2} \approx 65$ μas.

– (5) Modulation index $m_{\rm R}$
For the effective angular sizes obtained above, the modulation index $m_{\rm R}$ for the scintillating components can be derived as follows:

$$m_{\rm R} \approx 0.114\Big(\frac{\nu}{10\ {\rm GHz}}\Big)^{-2}\Big(\frac{\theta_{\rm eff}}{10\ \mu{\rm as}}\Big)^{-\frac{7}{6}} \times\Big(\frac{d}{\rm kpc}\Big)^{-\frac{1}{6}} SM^{0.5}. \quad (19)$$

We obtain $m_{\rm R,2}$ and $m_{\rm R,3}$ for the scintillating components S_2 and S_3 of ∼0.18 and ∼0.37 respectively. Thus, the flux density $S_{\rm c}$(mJy) at 20 cm of the scintillating components is obtained by:

$$S_{\rm c} \approx \frac{\sigma}{m_{\rm R}}. \quad (20)$$

They are $S_{\rm c,2} \approx 267$ mJy and $S_{\rm c,3} \approx 60.8$ mJy. Thus, the VLBI component-A contains a compact scintillating component S_3 with ∼20% ($\eta_{\rm c,3}$) of its flux density and the VLBI component-D contains a compact scintillating component with ∼67% ($\eta_{\rm c,2}$) of its flux density.

– (6) Apparent and intrinsic brightness temperatures
The apparent brightness temperature $T_{\rm b}\,({\rm K})$ for the scintillating components can be derived as follows:

$$T_{\rm b} \approx 0.49 \left(\frac{S_{\rm c}}{\rm mJy}\right)\left(\frac{\lambda}{\rm cm}\right)^2\left(\frac{\theta_{\rm s}}{\mu{\rm as}}\right)^{-2} 10^{12}\,. \qquad (21)$$

We obtain the apparent brightness temperature for the scintillating component S_2 and S_3 to be $T_{\rm b,2} \approx 3.7\,10^{12}$ K and $T_{\rm b,3} \approx 2.8\,10^{12}$ K respectively.

VLBI observations have shown that component-D shows superluminal motion with an apparent velocity $\sim 7.8\,c$ (c = speed of light; Hubble constant is assumed to be $H_0 = 100\,{\rm km\,s^{-1}\,Mpc^{-1}}$). If the viewing angle is assumed to be $\theta_{\rm v} \sim \frac{1}{\Gamma}$ (Γ = Lorentz factor of the superluminal motion), then the Doppler factor $\delta \approx 7.8$. Thus the intrinsic brightness temperature for the two scintillating components can be estimated:

$$T_{\rm b,int} \approx T_{\rm b}\,\delta^{-1}\,. \qquad (22)$$

(Since the angular sizes of the source components are derived from the scintillation theory, not from the causality effect, the transformation between the intrinsic and apparent brightness temperature only involves δ^{-1}). Thus we find $T_{\rm b,int,2}$ and $T_{\rm b,int,3}$ to be $4.7\,10^{11}$ K and $3.6\,10^{11}$ K. Both are significantly below the inverse-Compton limit ($\sim 10^{12}$ K).

All these values derived above are summarized in Table 1, in which $\theta_{\rm VLBI,6cm}$ denotes the angular size of the VLBI components measured at 6 cm.

In summary, in the three-component model, the VLBI component-D contains a very small subcomponent with an angular size of $\sim$0.12 mas and with $\sim$60% of its flux density at 20 cm. This subcomponent causes most of the scintillation. The VLBI component-A contains a subcomponent with an angular size of $\sim$0.065 mas and with only 13% of its flux density. This is consistent with the results given by Standke et al. (1996) in which component-A has an optically thick spectral index $\alpha_{\rm thick} < 2.5$ and could be a blend of inhomogeneous components which are not resolved. The scintillating component S_3 is the optically thick subcomponent at 20 cm.

The most interesting result may be that, for both the scintillating components, the derived intrinsic brightness temperatures are significantly below the inverse-Compton limit ($\sim 10^{12}$ K). This result is based on the adopted value for the Doppler factor $\delta \sim 7.8$, which is derived from the superluminal velocity observed for the VLBI component-D, assuming that the viewing angle is equal to $1/\Gamma \sim 7\overset{\circ}{.}3$ (where Γ– Lorentz factor of the motion). In other words, from the analysis of the intraday variations at 20 cm in the scintillation model presented here, the Doppler beaming factor in 0917+624 could still be quite large, i.e. both scintillation and Doppler beaming may be involved in the IDV phenomenon. Further VLBI observations would be desirable to check this result and would help to constrain the parameters of the interstellar medium.

Finally, we point out that even the proposed three-component model seems incapable of fully fitting the residual features in the polarization light curves, for example the feature at epoch JD2447651.75 (see Fig. 6). Such a feature could be due to another compact component scintillating with a timescale less than $\sim$0.2 days. However, some kind of low level intrinsic (intermittent) activity cannot be ruled out (Qian et al. 2000a,b).

Acknowledgements. We thank I. I. K. Pauliny-Toth and T. Beckert for critically reading the manuscript and valuable comments. We also thank the anonymous referee for enlightening suggestions. SJQ thanks the Max-Planck-Institut für Radioastronomie for hospitality and support during his visit.

References

Blandford, R., Narayan, R., & Romani, R. W. 1986, ApJ, 301, L53
Dennett-Thorpe, J., & de Bruyn, A. G. 2000, ApJ, 529, L65
Gabuzda, D. C., Kochanev, P. Yu., Cawthorne, T. V., & Kollgaard, R. I. 1999, in BL Lac Phenomenon, ed. L. O. Takalo, & A. Sillanpää, ASP, San Francisco, 447
Goodmann, J. 1997, New Astron., 2, 449
Heeschen, D. S., Krichbaum, T., Schalinski, C. J., & Witzel, A. 1987, AJ, 94, 1493
Kedziora-Chudzcer, L., Jauncey, D. L., Wieringa, M. H., et al. 1997, ApJ, 490, L9
Kellermann, K. I., & Pauliny-Toth, I. I. K. 1969, ApJ, 155, L71
Kochanev, P. Yu., & Gabuzda, D. C. 1998, in Radio Emission From Galactic and Extragalactic Compact Sources, ed. J. A. Zensus, G. B. Taylor, & J. M. Wrobel, ASP, San Francisco, p. 273
Kraus, A., Krichbaum, T. P., & Witzel, A. 1999, in BL Lac Phenomenon, ed. L. O. Takalo, & A. Sillanpää, ASP, San Francisco, 49
Krichbaum, T. P., Quirrenbach, A., Witzel, A., et al. 1992, in Variability in Blazars, ed. E. Valtaoja, & M. Valtonen (Cambridge Univ. Press, Cambridge), 331
Macquart, J. P., Kedziora-Chudczer, L., Rayner, D. P., & Jauncey, D. L. 2000, ApJ [astro-ph/0002192], in press
Marscher, A. P. 1996, in Proceedings of the Heidelberg Workshop on Gamma-ray Emitting AGN, ed. J. G. Kirk, M. Camenzind, C. von Montigny, & S. Wagner, MPIfK, Heidelberg, 103
Marscher, A. P. 1998, in Radio Emission From Galactic and Extragalactic Compact Sources, ed. J. A. Zensus, G. B. Taylor, & J. M. Wrobel, ASP, San Francisco, 25
Narayan, R. 1992, Phil. Trans. R. Soc. Lond. A, 341, 151
Qian, S. J., Quirrenbach, A., Witzel, A., et al. 1991, A&A, 241, 15
Qian, S. J., Britzen, S., Witzel, A., et al. 1995, A&A, 295, 47
Qian, S. J. 1994 a, Acta Astron. Sin., 35, 362 (Transl.: Chin. Astron., 1995, 19, 267)
Qian, S. J. 1994 b, Acta Astrophys. Sin., 14, 333 (Transl.: Chin. Astron., 1995, 19, 69)
Qian, S. J., Li, X. C., Wegner, R., et al. 1996, Chin. Astron., 20, 15
Qian, S. J., & Zhang, X. Z. 1996, Acta Astron. Sin., 37, 421 (Transl.: Chin. Astron., 1997, 21, 162)

Qian, S. J., Kraus, A., Witzel, A., et al. 2000a, A&A, 357, 84
Qian, S. J., Kraus, A., Krichbaum, T. P., et al. 2000b, in Proceedings of IAU Colloquium 182, April 2000, Quiyang, China, in press
Quirrenbach, A., Witzel, A., Krichbaum, T. P., et al. 1992, A&A, 258, 279
Quirrenbach, A., Witzel, A., Qian, S. J., et al. 1989, A&A, 226, L1
Quirrenbach, A., Kraus, A., Witzel, A., et al. 2000, A&AS, 141, 221
Rickett, B. J. 1990, ARA&A, 28, 561
Rickett, B. J., Quirrenbach, A., Wegner, R., et al. 1995, A&A, 293, 479
Romero, G. E., Combi, J. A., Benaglia, P., et al. 1997, A&A, 326 77
Spada, M., Salvati, M., & Pacini, F. 1999, ApJ, 511, 136
Standke, K. J., Quirrenbach, A., Krichbaum, T. P., et al. 1996, A&A, 306, 27
Wagner, S., & Witzel, A. 1995, ARA&A, 33, 163
Wagner, S. J., Witzel, A., Heidt, J., et al. 1996, AJ, 111, 2187
Witzel, A. 1992, in Physics of Active Galactic Nuclei, ed. W. J. Duschl, & S. Wagner (Springer, Heidelberg), 484